Modeling Contaminant Adsorption in Packed Columns using Nonlinear Mass Transfer

---

Master's Degree Dissertation

Professor:

Tim Myers

Author:

Albert Estop

July, 2023

Abstract

This project focuses on the modeling of the adsorption process in packed columns, a widely employed method for removing contaminants from fluids. A mathematical model is developed to describe the flow of fluid through the porous media of a packed column, while contaminants are removed. This work employs a nonlinear model for the mass transfer process and unlike previous studies, considers non-constant fluid velocity. After non-dimensionalising the system, an analytical traveling wave solution is obtained. With this solution we can determine the fluid components concentration, remaining adsorbent, fluid velocity, and pressure at any position within the column for the whole process. To estimate its validity, the model's performance is evaluated through two different experiments, toluene adsorption on activated carbon and CO_2 adsorption on activated carbon. Comparison with the data from the first experiment is used to test the model and check if it satisfies the model assumptions keeping constant the adsorption coefficient. In the second experiment a larger amount of contaminant is removed and the model is validated in a variable velocity system. Simpler models are finally considered and compared with the model developed.

Contents

1 Introduction

It goes without saying that humanity is starting to kill this planet. Air pollution is raising the Earth's temperature faster than ever, causing the rise of the mean sea levels and increasing the frequency of natural disasters. All these changes are now affecting directly life in many places, causing more than the 11% of global deaths [1]. Not to mention the impact that this is having in nature. Oceans are acidifying due to CO_2 melting mollusks shells [2]. According to IUCN (International Union for Conservation of Nature), around 10% of all marine species are at risk of extinction, 45% of them because of climate change, facing the biggest extinction in 250 million years. The conjecture that everything will probably escalate to a critic and direct thread is increasingly recurrent.

Reducing pollutants in both air and water is an urgent priority. As trying to reduce consumption is clearly not enough active removal of contaminants should be performed. Column sorption is the most used sorption method to filter contaminated fluids [3], used to remove CO_2, chemicals and salts among others. The process consists on forcing the fluid through a tube filled with sorbent, a porous material equally distributed in the tube that will remove certain components of the fluid. Initially the contaminant is removed in the inlet region. As sorbent wears out the main region where the sorption process occurs travels forward. Eventually the sorbent saturates and the fluid will pass through unchanged. These contaminants can be removed by absorption, entering inside the absorbent, or adsorption, attaching to the adsorbent's surface.

Due to the current need to use and improve these technologies, there is a vast literature on the subject including experimental, computational and theoretical studies. Experimental studies provide data used later to develop and test models developed in computational and theoretical studies. Computational studies are proved to work effectively, although it is difficult to infer their physical operating conditions. Theoretical studies try to mathematically model the process based on simplified systems, providing approximated results but well physically contextualized. However, the modeling of the adsorption process has proven to be a factor leading to significant inconsistencies within model predictions and experimental results, as they lead to constants that change with contaminant concentration [4]. Consequently, different approaches to represent this phenomena have arisen among the literature. Some are simply based on the probability of a contaminant molecule escaping while the more recent ones try to reproduce the physical process that occurs along the column, see 2.2. They all focus in the prediction of breakthrough curves, which is the evolution of contaminant concentration at the outlet of the column, as it is usually the data provided by experimental results and therefore the easiest way to compare the model accuracy.

In this project a model to describe a two-component gas flowing through a packed column is developed, where the contaminant will be removed by adsorption. Mass transfer process has been represented using the Langmuir nonlinear equation, explained in detail in Section 2.2. This approach to model adsorption has been proven to work satisfactorily, predicting with accuracy experimental results in different studies. In addition, the model considers variable fluid velocity and a solution for its evolution is developed. This, combined with the Langmuir nonlinear equation had not been done before.

Parameters that characterize a real system can exhibit significant variation. To ensure the robustness and versatility of our model across various scenarios, we will evaluate its performance using two distinct experimental datasets. The first one contains the results of toluene adsorpion in activated carbon. This experiment was performed for three different inlet contaminant concentrations, and after determining the missing parameters by fitting the model to the experimental data, we will see if coherent results are obtained. The second experiment is CO_2 adsorption in activated carbon. Contaminant concentrations in the first experiment are very

small and therefore the velocity gradient will not be appreciable. In the second case the contaminant concentration is much higher and we will use it to check if the model performs accurately in a variable velocity system, and compare it with a constant velocity one to see if results obtained with the model developed are indeed more accurate.

2 Derivation of governing equations

In this section we will develop and present the governing equations of the mathematical system used to model the adsorption process in a packed column. Our goal is to determine the sorbed mass at any given moment in time, and thus derive the contaminant concentration at the outlet of the column for the whole process. Therefore we will not delve into modelling the fluid dynamics beyond what is necessary to compute the quantities we are interested in. The following assumptions have been done when developing the model:

- The inlet gas is formed by two components, the contaminant and the carrier.
- The gas follows plug flow, meaning that as the inside shape of the column is not known we will perform a radial averaging reducing the system to one dimension. Consequently space is reduced to one dimension and variables will only depend on x, representing the coordinate along the column axis, and t.
- Temperature, T, the initial concentration of the gas components, c_{10} and c_{20}, ambient pressure, p_a and initial interstitial velocity, u_0, are maintained constant during the experiment.

2.1 Continuity equation

In the physical system considered there is fluid passing through a packed column, which is assumed to be hermetical. Therefore, the only source of mass loss will be the contaminant removal due to the sorption process. In this context, we will use the mass continuity equation to mathematically model this phenomena. For the flow of a fluid without mass transfer, this equation can be written as:

$$\frac{\partial \rho}{\partial t} + \nabla \cdot \mathbf{j} = 0, \tag{1}$$

where ρ is the density of the fluid. If we now consider mass loss due to the sorption process we have to add another term to the expression:

$$\frac{\partial \rho}{\partial t} + \nabla \cdot \mathbf{j} = -S. \tag{2}$$

S is the sink term representing the mass loss. The flux $\mathbf{j}$ is given by the following expression:

$$\mathbf{j} = -D\nabla\rho + \rho\mathbf{u} \tag{3}$$

where the first term corresponds to the flux originated by diffusion and the second term is the flux corresponding to the fluid traveling through the packed column. As it was mentioned before the shape of the porous media of the packed column is not known so plug flow is assumed. Hence, the fluid velocity can be written as $\mathbf{u} = (u(x,t), 0)$. In [5] the sink term is developed following this assumption, obtaining:

$$s = (1-\varepsilon)\rho_q M_q \frac{\partial \overline{q}}{\partial t} \tag{4}$$

where ε is the bed void fraction, ρ_q is the contaminant density and M_q is the molar mass of the adsorbed material. $\frac{\partial \overline{q}}{\partial t}$ is the adsorption rate, where $\overline{q}$ represents the total amount of material adsorbed. Introducing everything into Eq. (2) mass continuity equation now reads:

$$\frac{\partial \rho}{\partial t} + \frac{\partial (u\rho)}{\partial x} = D\frac{\partial^2 \rho}{\partial x^2} - (1-\epsilon)\rho_q M_q \frac{\partial \bar{q}}{\partial t} \tag{5}$$

2.2 Mass transfer equation

To model the rate at which contaminant is removed in the column we will introduce a mass transfer equation. Its solution will complement the continuity equation defining the contaminant concentration gradient at each time instant.

As previously mentioned in the introduction, the mathematical formulation of mass transfer can lead to inconsistencies in packed column models. To solve the problem different approaches have arisen to represent the process. Simpler models based on the probability of adsorption or breakthrough conclude that $q_t(L,t) \propto c(L,t)(c_{in} - c(L,t))$, where q_t is the adsorbed quantity variation, $c(L,t)$ is the fluid concentration at the outlet of the column and c_{in} is the inlet fluid concentration. On the other hand, in models that try to reproduce the physical process that occurs along the column the adsorbent is thought to be an ideal surface with independent sites that hold the contaminant molecules, which attach to it forming a one molecule layer around it. Therefore the adsorption rate will be proportional to the contaminant concentration, c_1, together with the adsorption capacity left on the adsorbent material, $\bar{q}^* - \bar{q}$, leading to $q_t \propto c(x,t)(\bar{q}^* - \bar{q})$, where $\bar{q}^*$ is the saturation value of the adsorbent. In both cases the constant of proportionality relating the mass transfer velocity q_t with the different expressions is the adsorption coefficient k_{ad}, which is the origin of inconsistencies arising in packed column models. As the value of this parameter is not known, it is determined by fitting the breakthrough curve solution to the one obtained experimentally. However, if the procedure is performed with different experimental datasets, it is usually determined that k_{ad} varies with the inlet concentration of contaminant, conflicting with the premise that the coefficient was constant.

In this work we have used the Langmuir equation to model the process. This approach additionally takes into account desorption, which can be understood as the phenomenon when the fluid drags away particles already attached to the adsorbent. Therefore a new term proportional to the adsorbed quantity $\bar{q}$ is included in the mass transfer rate, which reads:

$$\frac{\partial \bar{q}}{\partial t} = k_{ad} c_1 \left(\bar{q}^* - \bar{q}\right) - k_{de} q, \tag{6}$$

where k_{de} is the desorption rate constant and c_1 is the contaminant concentration. This model is referred as the nonlinear model, as it contains a $c\bar{q}$ term, to differentiate it from its linear approximation (see [4]) often used to make its analysis easier. This linear model only depends on the adsorption capacity, $\bar{q}^* - \bar{q}$. During the initial transient, the adsorbent at the inlet of the column will remove the contaminant in the fluid until saturating. Then the further the contaminant travels through the column the more adsorption capacity the adsorbent will have and the less contaminant will remain in the fluid. Eventually the contaminant will be completely removed, resulting in a similar profile as the one given in Figure 1a. However, this model will only hold in regions where there is contaminant to adsorb. In regions of the column where the contaminant has not yet reached, adsorbed quantity will be zero $\bar{q} = 0$. Therefore, the adsorption rate given by this model will be very high. This is clearly wrong as the column can not adsorb contaminant if there isn't any.

The nonlinear model on the other hand, takes into consideration contaminant concentration in the fluid. This corrects the inconsistency of the linear model, as in regions where there is no contaminant the adsorption rate will be zero. Including the concentration term will also smooth the adsorption profile (see Figure 1b), as in regions where there is very little contaminant adsorption rate will reduce proportionally, never letting the concentration reach zero.

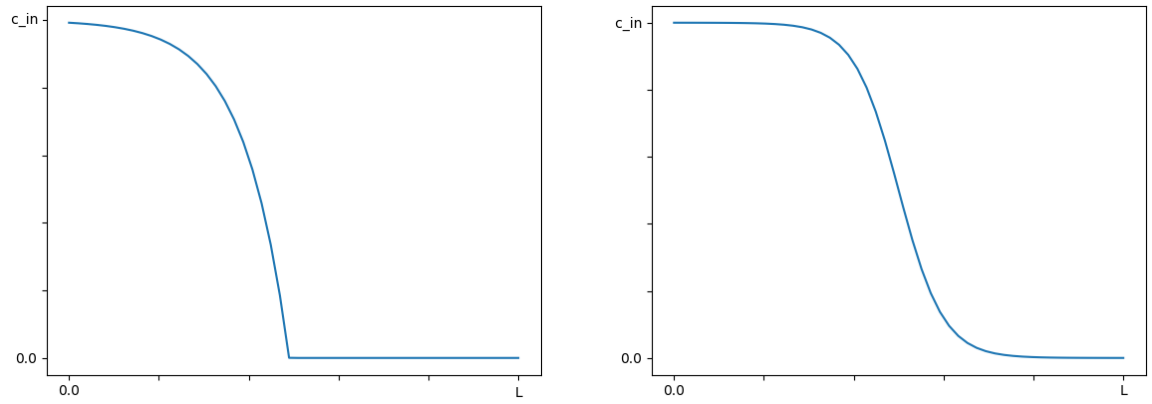

(a) Linear sink model **(b)** Nonlinear sink model

Figure 1: Plots of typical contaminant concentration profiles through the column for a given time.

2.3 Ideal gas law

If we have constant fluid velocity [4], the system would be fully described by above equations. This case could be applied when the contaminant volume fraction is small, as the fluid volume gradient originated by the contaminant adsorption would be negligible and p and u would remain constant. When the contaminant volume fraction is significant, pressure and fluid velocity are not constant anymore, so we need two more equations to describe the system, which now has two more variables. The first of them is obtained from the ideal gas law, which relates pressure with concentration, although it will only hold at low temperatures:

$$p = R_g T c \tag{7}$$

2.4 Momentum equation

As it was said above, as fluid velocity may be variable, we need two more equations apart from the mass transfer and the continuity equation to model the evolution the variables that describe the system. The last relation needed will be derived from the Navier-Stokes equation. This equation models the fluid dynamics occurring inside the column by computing the momentum of the fluid. Following the plug flow assumption and therefore reducing the system to one dimension, N-S equation can be reduced to:

$$\rho\left(\frac{\partial u}{\partial t} + u\frac{\partial u}{\partial x}\right) = -\frac{\partial p}{\partial x} + \frac{4}{3}\mu\frac{\partial^2 u}{\partial x^2} - Su, \tag{8}$$

where Su is the momentum loss due to mass reduction and the factor $4/3$ multiplying the second term in the right hand side of the equation represents is specific for compressible fluids.

When considering the steady flow of an incompressible fluid, the factor $4/3$ becomes unity. In this context $S = 0$, and u_t, u_x factors can be neglected, as u will take a very small value. Considering these changes and assuming that viscous resistance is proportional to velocity $u_{xx} \propto u$, Eq.(8) reduces and we obtain Darcy's law, which describes the flow of an incompressible liquid through pores considering viscous resistance:

$$-\frac{\partial p}{\partial x} = \frac{\mu}{k_p} u, \tag{9}$$

where k_p is the permeability.

However, in gases viscous resistance is very low and inertial resistance should be considered. To describe it we use a drag law:

$$u\frac{\partial u}{\partial x} = C_D \frac{u^2}{d} \tag{10}$$

where d is the length-scale and $C_D = C_D(\epsilon, Re, d)$ the drag coefficient. We can use this expression to obtain a relation between pressure gradient and velocity, as done when deriving Darcy's law:

$$F = \rho \frac{u^2}{d} C_D. \tag{11}$$

We also have to include one last term regarding the sink term proportional to the velocity. Combining all three we finally obtain the momentum equation, which relates the pressure and the velocity of the fluid:

$$-\frac{\partial p}{\partial x} = \alpha \rho u^2 + \left(\beta + (1-\epsilon)\rho_q M_1 \frac{\partial \bar{q}}{\partial t}\right) u, \tag{12}$$

where α and β are constants and M_1 is the contaminant molar mass. By observing the equation we can see that momentum loss might occur in the region where the major part of the mass transfer is occurring. There the sink term will be higher and the velocity will probably reduce to match the pressure gradient, probably inducing momentum loss.

2.5 Two-component fluid

As we have assumed that the inlet gas is formed by two components, we can write $\rho = M_1 c_1 + M_2 c_2$, where M_1, M_2 are the molar masses of the gas contaminant and carrier respectively, and c_1, c_2 are their concentrations in mols/m^3. Introducing this change the governing equations can be rewritten as:

$$\begin{cases} \frac{\partial c_1}{\partial t} + \frac{\partial}{\partial x}(u c_1) = D\frac{\partial^2 c_1}{\partial x^2} - (1-\varepsilon)\rho_q \frac{M_q}{M_1}\frac{\partial \bar{q}}{\partial t} \\ \frac{\partial c_2}{\partial t} + \frac{\partial}{\partial x}(u c_2) = D\frac{\partial^2 c_2}{\partial x^2} \end{cases} \tag{13}$$

$$\frac{\partial \bar{q}}{\partial t} = k_{ad} c_1 \left(\bar{q}^* - \bar{q}\right) - k_{de} q, \tag{14}$$

$$p = R_g T \left(c_1 + c_2\right) \tag{15}$$

$$-\frac{\partial p}{\partial x} = \alpha(M_1 c_1 + M_2 c_2)u^2 + \left(\beta + (1-\epsilon)\rho_q M_1 \frac{\partial \bar{q}}{\partial t}\right) u \tag{16}$$

With these five equations the evolution of the five variables that characterize the state of the system, $c_1, c_2, u, p, \bar{q}$, is fully described.

2.6 Boundary and initial conditions

As we can see above, we have a differential system of equations that will be solved by integrating, so we need to specify the boundary and initial conditions that we will later use to find the values of the integrating constants.

Following from the assumption that there will be a steady gas flow at the inlet of the column, we can derive that just before and after the inlet $x = 0$ the velocity of the whole fluid, u, will be respectively:

$$\begin{cases} u(0^-, t) = \frac{Q_0}{\pi R^2} \\ u(0^+, t) = \frac{Q_0}{\varepsilon \pi R^2} \end{cases} \tag{17}$$

At the extremes of the column there is no mass transfer. Therefore we can write the following mass flux and concentration constraints:

$$u(0^-, t)c_{10} = \left(uc_1 - D\frac{\partial c_1}{\partial x} \right)\Big|_{x=0^+}, \tag{18}$$

$$u(0^-, t)c_{20} = \left(uc_2 - D\frac{\partial c_2}{\partial x} \right)\Big|_{x=0^+}, \tag{19}$$

$$\frac{\partial c_1}{\partial x}\Big|_{x=L^-} = \frac{\partial c_2}{\partial x}\Big|_{x=L^-} = 0. \tag{20}$$

Boundary conditions regarding pressure are:

$$p(0, t) = p_0(t), \quad p(L, t) = p_a \tag{21}$$

As we can see pressure at $x = 0$ is expressed as a function of time to keep the model general. If we have an experiment with constant inlet pressure, this expression should be replaced by its value. However if we have constant inlet flux instead, then pressure at the inlet of the column will be variable as it will also depend on the quantity of contaminant being adsorbed at the inlet.

As it is later explained (see Section 4), as fluid passes through the column the adsorbent wears out and the main region where the contaminant is removed moves forward. Eventually the column saturates and the fluid emerges unchanged. As mass transfer Eq. (6) depends on the contaminant concentration, diffusion is taken in to account. This means that a fraction of contaminant will travel forward in the column much faster than u, hence in the area beyond the main sorption region contaminant concentration will tend towards zero without reaching it, $c_1 \to 0$. Following this reasoning we can state

$$\begin{gathered} c(x, t),\ \overline{q}(x, t) \to 0, \quad \text{as} \quad t \to -\infty \\ c(x, t) \to c_{10}, \quad \overline{q}(x, t) \to \overline{q}_e, \quad \text{as} \quad t \to \infty, \end{gathered} \tag{22}$$

where q_e is defined as the equilibrium adsorbed mass. It may be clear to think that for $t \to \infty$ the adsorbent will saturate reaching $\overline{q} \to \overline{q}_0^*$. However, when $\overline{q}$ is reaching $\overline{q}_0^*$ adsorption rate will be very small. As our mass transfer equation considers desorption, before the sorbent saturates there will be a point when mass will be adsorbed and desorbed at the same rate and therefore no mass transfer will take place. At this point the adsorbed mass will remain constant and we will define this equilibrium value as $\overline{q}_e$.

Finally as we have assumed that initially the fluid is free of contaminant. Therefore, the initial conditions are:

$$p(x,0) = M_2 c_2(x,0) = M_2 \frac{p(x)}{RT}, \quad q(x,0) = 0$$
$$\Rightarrow c_1(x,0) = 0, \quad c_2(x,0) = \frac{p_{in}(x)}{RT}, \tag{23}$$

where $p_{in}(x) = p_0(0) - (p_0(0) - p_a)x/L$.

2.7 Determination of adsorption and desorption parameters

All parameters introduced above are assumed to be given together with experimental data. However, k_{ad} and k_{de} are hard to determine and they are usually unknown. Their value may depend on certain system parameters, such as pressure, temperature or flow rate, but as they are introduced as constants within the Langmuir equation Eq. (6), they should not depend on c_1 and $\overline{q}$. We can rearrange Eq. (6) as

$$\frac{\partial \overline{q}}{\partial t} = k_{ad} c \left(1 + \frac{1}{k_L c}\right)\left(\frac{\overline{q}^* k_L c}{1 + k_L c} - q\right), \tag{24}$$

where $k_L = k_{ad}/k_{de}$ is the Langmuir constant.

As it was explained above, when fluid goes through the column adsorbed mass increases until it starts approaching its saturation value. Eventually adsorption and desorption rates equalize, as they are proportional to $\overline{q}^* - \overline{q}$ and $\overline{q}$ respectively. At this point an equilibrium is reached where the fluid passing through the column remains unchanged and adsorbed quantity remains constant. The boundary conditions at this equilibrium point are defined in Eq.(22) for $t \to \infty$. Introducing them in the rearranged mass transfer equation Eq. (24) we can compute the so called Langmuir isotherm:

$$\overline{q}_e = \frac{\overline{q}^* k_L c_{10}}{1 + k_L c_{10}}, \tag{25}$$

If we compute the inverse of the function we obtain:

$$\frac{1}{\overline{q}_e} = \frac{1}{\overline{q}^*} + \frac{1}{k_L \overline{q}^*}\frac{1}{c_{10}}, \tag{26}$$

This expression is equivalent to line function, where $1/\overline{q}_e$ is the y-coordinate and $1/c_{10}$ the x-coordinate. If we have the data of an experimental study for more than one inlet concentration, we can determine one $(\frac{1}{c_e}, \frac{1}{q_e})$ point for each experiment and compute a regression line to find the values of $\overline{q}^*$ and k_L. $k_a d$ will be finally determined fitting the solution of Eq. (25) to the experimental data, since it will be the only parameter missing. Following from the definition of k_L, k_{de} will be simultaneously determined with k_{ad}.

Experimentally, $\overline{q}_e$ can be determined by computing the difference between the initial and final weight of material in the column

$$\overline{q}_e = \frac{M_f - M_i}{M_i}. \tag{27}$$

M_i is the mass inside the column at the beginning of the process and M_f the mass in the column once equilibrium has been reached. The experimental that we usually have is the evolution of the contaminant concentration at the outlet of the column. With this data we can compute $\overline{q}_e$ performing the numerical integration of the contaminant that remains in the column each iteration:

$$\overline{q}_e = \frac{1}{M_i}\int_0^{\infty} J_{in}(c_e - c_1)dt \approx \frac{J_{in}}{2M_i}\sum_{i=1}^{N}(2c_e - c_i - c_{i-1})(t_i - t_{i-1}), \tag{28}$$

where $c_e = c_{10}$. N is the number of experimental data points available, and c_i is the contaminant concentration at the outlet of the column measured the time i, where $i = 0$ corresponds to the first measurement performed.

3 Non-dimensionalisation

The system of equations that model the column will probably need to be solved numerically. Therefore, as it is usually done in numerical problems the system will be non-dimensionalized to simplify the problem and reduce the error of the solution. To perform the non-dimensionalisation we have followed an analog procedure to the one performed in [6]. However, as we are using the nonlinear Langmuir equation to model the mass adsorption process, we have obtained a different non-dimensional mass transfer equation, and introduced a new non-dimensional parameter δ_9 defined below.

The new dimensionless variables would be defined as:

$$\begin{gathered}\hat{p} = \frac{p - p_a}{\Delta p}, \quad \hat{c}_1 = \frac{c_1}{c_{10}}, \quad \hat{c}_2 = \frac{c_2}{c_{20}}, \quad \hat{q} = \frac{\bar{q}}{\bar{q}_0^*} \\ \hat{x} = \frac{x}{\mathcal{L}}, \quad \hat{t} = \frac{t}{\Delta t}, \quad \hat{u} = \frac{u}{u_0},\end{gathered} \tag{29}$$

where

$$\Delta t = 1/(k_{ad} c_{10}), \quad \mathcal{L} = u_0 c_{10}/((1-\varepsilon)\rho_q \overline{q}_0^* k_{ad} c_{10}), \quad \Delta p = \beta u_0 \mathcal{L} \tag{30}$$

where $\overline{q}^*$ is the value of $\overline{q}^*$ at $t = 0$. $\mathcal{L}$ is defined to to reflect the main reaction range rather than the length of the column.

After introducing the change of variables we obtain the corresponding dimensionless equations:

$$\delta_1 \frac{\partial \hat{c}_1}{\partial \hat{t}} + \frac{\partial}{\partial \hat{x}}\left(\hat{u}\hat{c}_1\right) = \delta_2 \frac{\partial^2 \hat{c}_1}{\partial \hat{x}^2} - \frac{\partial \hat{q}}{\partial \hat{t}} \tag{31}$$

$$\delta_1 \frac{\partial \hat{c}_2}{\partial \hat{t}} + \frac{\partial}{\partial \hat{x}}\left(\hat{u}\hat{c}_2\right) = \delta_2 \frac{\partial^2 \hat{c}_2}{\partial \hat{x}^2} \tag{32}$$

$$\frac{\partial \hat{q}}{\partial \hat{t}} = \hat{c}_1\left(\hat{q}^* - \hat{q}\right) - \delta_9 \hat{q} \tag{33}$$

$$1 + \delta_3 \hat{p} = \delta_4\left(\hat{c}_2 + \delta_5 \hat{c}_1\right) \tag{34}$$

$$-\frac{\partial \hat{p}}{\partial \hat{x}} = \delta_6\left(\hat{c}_2 + \delta_7 \hat{c}_1\right)\hat{u}^2 + \left(1 + \delta_8 \frac{\partial \hat{q}}{\partial \hat{t}}\right)\hat{u} \tag{35}$$

where we have assumed that $c_{10} < c_{20}$ in the fourth equality.

Boundary and initial conditions are:

$$1 = \left(\hat{u}\hat{c}_1 - \delta_2 \frac{\partial \hat{c}_1}{\partial \hat{x}}\right)\Big|_{\hat{x}=0^+}, \quad 1 = \left(\hat{u}\hat{c}_2 - \delta_2 \frac{\partial \hat{c}_2}{\partial \hat{x}}\right)\Big|_{x=0^+}, \tag{36}$$

$$\left.\frac{\partial \hat{c}_1}{\partial \hat{x}}\right|_{\hat{x}=\hat{L}^-} = \left.\frac{\partial \hat{c}_2}{\partial \hat{x}}\right|_{\hat{x}=\hat{L}^-} = 0, \quad \hat{p}(0,\hat{t}) = \hat{p}_0(\hat{t}) \quad \hat{p}(\hat{L}) = 0, \tag{37}$$

$$\hat{c_1}(\hat{x},0) = 0, \quad \delta_4 \hat{c}_2(\hat{x},0) = 1 + \delta_3 \hat{p}_{in}, \quad \hat{q}(\hat{x},0) = 0, \tag{38}$$

$$\begin{gathered}\hat{c}(\hat{x},\hat{t}),\ \hat{q}(\hat{x},\hat{t}) \to 0, \quad \text{as} \quad \hat{t} \to -\infty, \\ \hat{c}(\hat{x},t),\ \hat{q}(\hat{x},\hat{t}) \to \hat{q}_e, \quad \text{as} \quad \hat{t} \to \infty,\end{gathered} \tag{39}$$

where the initial pressure is $\hat{p}_{in} = \hat{p}_0(0)(1 - \hat{x}/\hat{L})$.

The non-dimensional parameters δ_i left in the dimensionless equations are:

$$\delta_1 = \frac{\mathcal{L}k_{ad}c_{10}}{u_0} = \frac{c_{10}}{(1-\varepsilon)\rho_q \overline{q}_0^*}, \quad \delta_2 = \frac{D}{\mathcal{L}u_0}, \quad \delta_3 = \frac{\Delta p}{p_a}, \quad \delta_4 = \frac{R_g T c_{20}}{p_a}, \quad \delta_5 = \frac{c_{10}}{c_{20}},$$
$$\delta_6 = \frac{\alpha M_2 c_{20} u_0^2 \mathcal{L}}{\Delta p} \quad \delta_7 = \frac{M_1 c_{10}}{M_2 c_{20}}, \quad \delta_8 = \frac{1-\varepsilon}{\beta}\rho_q M_1 \overline{q_0}^* k_{ad} c_{10}, \quad \delta_9 = \frac{k_{de}}{k_{ad}c_{10}} = \frac{1}{k_L c_{10}}$$

3.1 Physical reduction of the system

The dimensionless equations may be solved numerically. However, we can simplify the equations by neglecting the lower-order parameters, since their impact in the evolution of the variables that define the system will be negligible. By introducing a change of variables, an analytical traveling wave solution of the reduced system may be found. This will provide the advantages and disadvantages of theoretical solutions such as the clear derivation of the system dependencies at the cost of having an approximated solution.

In constant velocity models the parameter $\overline{q}^*$ is usually taken as constant. Therefore it can be canceled out when changing to dimensionless form as $\hat{q}^* = \overline{q}^*/\overline{q}^* = 1$. However, using the kinetic model described in [7] we see that it depends on p

$$\overline{q}^* = \frac{q_{m1}K_{T1}p}{\left[1+(K_{T1}p)^{n1}\right]^{1/n1}} + \frac{q_{m2}K_{T2}p}{\left[1+(K_{T2}p)^{n2}\right]^{1/n2}}. \tag{40}$$

As in our model the fluid velocity u is assumed to be variable, p will also be variable and we can not perform the reduction of this term. If we express it in non-dimensional form we obtain

$$\begin{aligned}\hat{q}_0^* = \overline{q}_0^*\hat{q} = &\frac{q_{m1}K_{T1}p_a\left(1+\delta_3\hat{p}\right)}{\left[1+\left(K_{T1}p_a\left(1+\delta_3\hat{p}\right)\right)^{n1}\right]^{1/n1}} \\ &+ \frac{q_{m2}K_{T2}p_a\left(1+\delta_3\hat{p}\right)}{\left[1+\left(K_{T2}p_a\left(1+\delta_3\hat{p}\right)\right)^{n2}\right]^{1/n2}},\end{aligned} \tag{41}$$

where $\hat{p}$ is always accompanied by δ_3. Recalling the definition of δ_3, we can see observe that as experimental studies are usually performed at ambient pressure the value of the parameter p_a will move around $p_a \sim 10^6$. On the other hand Δp will generally have a value of order $\Delta p \sim 10^1$, so we can neglect $\delta_3 = \Delta p/p_a$ which will be of order $\delta_3 \sim 10^{-4}$. With this reduction $\overline{q}_0^*$ loses its p dependency becoming constant. It can be then canceled out as in constant velocity models $\hat{q}^* = \overline{q}^*/\overline{q}_0^* = \overline{q}^*/\overline{q}^* = 1$.

Considering that the contaminant comprises less than the 25% of the fluid, its concentration will be of order $c_1 < 10^1$. If this assumption holds, we will neglect δ_1, which will have a value of order $\delta_1 \sim 10^{-2}$. Finally, we will also neglect δ_2, as diffusion is usually very small making this dimensionless constant of the same order as δ_1, $\delta_2 \sim 10^{-2}$.

For cases where the concentration of contaminant in the fluid is significant, the leading term in Eq. (35) will be δ_7. The other two dimensionless parameters of the equation δ_6 and δ_8 will generally be of lower order and therefore neglected. If the concentration of contaminant is low, δ_7 will also be small and we will be able to neglect it as well. However, as δ_7 only appears multiplying δ_6, the obviation of the second one implies the obviation of the first, so δ_7 will not be relevant regardless the contaminant concentration.

Introducing these reductions in the dimensionless system, we can rewrite it as:

$$\frac{\partial}{\partial \hat{x}}\left(\hat{u}\hat{c}_1\right) = -\frac{\partial \hat{q}}{\partial \hat{t}} \tag{42}$$

$$\frac{\partial}{\partial \hat{x}}\left(\hat{u}\hat{c}_2\right) = 0 \tag{43}$$

$$\frac{\partial \hat{q}}{\partial \hat{t}} = \hat{c}_1\left(1-\hat{q}\right) - \delta_9 \hat{q} \tag{44}$$

$$1 = \delta_4\left(\hat{c}_2 + \delta_5 \hat{c}_1\right) \tag{45}$$

$$-\frac{\partial \hat{p}}{\partial \hat{x}} = \hat{u}\ . \tag{46}$$

As it can be observed, we now have $\hat{c}_1$ and $\hat{c}_2$ directly related by Eq. (45). As it is performed in next section, Eq.(43) can be directly integrated obtaining a relation between $\hat{c}_2$ and $\hat{u}$, and combining both equalities we can also relate $\hat{c}_1$ and $\hat{u}$. This new relation eliminates the dependence of Eq. (42) on $\hat{u}$. Consequently, both Eq. (42) and Eq. (44) now depend on $\hat{q}$ and $\hat{c}_1$, and can be solved as performed in constant fluid velocity models. After finding a solution, $\hat{p}$ will be finally determined using Eq. (46).

4 Mathematical solutions

As it is explained above, after introducing the physical reductions in the dimensionless system, we can relate the variables until reducing the problem to a two equation system, with variables $\hat{c}_1$ and $\hat{q}$. Once we obtain this, we can develop a traveling wave analytical solution. In this section this solution is developed, and the equations that will govern the evolution of the model are presented.

4.1 Traveling wave solution

Initially, the fluid is filtered at the inlet of the packed column. As adsorbent is filled with contaminant it loses effectiveness and the main area where the mass transfer process occurs moves forward as fluid passes though. Once the initial transient is completed, this main reaction front keeps its shape while moving, behaving as a traveling wave. Following this reasoning we can develop an analytical traveling wave solution, as performed in [6].

By neglecting δ_1 and δ_2 from Eq. (43), we obtain a ODE that we can solve directly by integrating, obtaining:

$$\hat{u}\hat{c}_2 = 1 \tag{47}$$

Combining this result with Eq. (42), we can obtain an explicit expression of the interstitial velocity in terms of the contaminant concentration $\hat{u} = \hat{u}(\hat{c}_1) = 1/(1 - \delta_{45}\hat{c}_1)$. This lets us remove $\hat{u}$ from the contaminant mass continuity relation Eq. (42), which can be rewritten as:

$$\delta_4 \frac{\partial}{\partial \hat{x}} \left(\frac{\hat{c}_1}{1 - \delta_{45}\hat{c}_1} \right) = -\frac{\partial \hat{q}}{\partial \hat{t}}, \tag{48}$$

where $\delta_{45} = \delta_4\delta_5$. We can solve this equation together with Eq. (44) obtaining $\hat{c}_1(x,t)$ and $\hat{q}(x,t)$, and then use previous equations to obtain the remaining variables $\hat{u}, \hat{p}, \hat{c}_2$.

To obtain the solution we will first choose a new coordinate origin that will travel with the wave front $\eta = \hat{x} - \hat{s}(\hat{t})$, where $\hat{s}(\hat{t})$ is the wave front position. As explained in Section 2.2, $\hat{c}_1$ never actually reaches $\hat{c}_1 = 0$ due to the c_1 term in the nonlinear mass transfer equation. Therefore, we will take as wave front the point $\eta = 0$, the coordinate where $\hat{c}_1 = 1/2$. We will also introduce a new variable to simplify Eq. (48), defined

$$\hat{f} = \hat{u}\hat{c}_1 = \frac{\delta_4 \hat{c}_1}{1 - \delta_{45}\hat{c}_1}. \tag{49}$$

By implementing these transformations, we can rewrite Eqs. (48, 44) as:

$$\frac{\partial \hat{f}}{\partial \hat{\eta}} = \hat{s}_{\hat{t}} \frac{\partial \hat{q}}{\partial \hat{\eta}}, \tag{50}$$

$$-\hat{s}_{\hat{t}} \frac{\partial \hat{q}}{\partial \hat{\eta}} = \hat{c}_1(1 - \hat{q}) - \delta_9 \hat{q}, \tag{51}$$

where $\hat{s}_{\hat{t}}$ is the velocity of the wave front. Introducing the new variables in Eq. (39) we obtain the boundary conditions for above equations:

$$\hat{f},\ \hat{c}(\eta),\ \hat{q}(\eta) \to 0,\ \hat{c}',\ \hat{f}',\ \hat{q}' \to 0, \quad \text{as} \quad \eta \to \infty,$$

$$\hat{f},\ \hat{c}(\eta) \to 1,\ \hat{q}(\eta) \to \hat{q}_e,\ \hat{c}',\ \hat{f}',\ \hat{q}' \to 0, \quad \text{as} \quad \eta \to -\infty. \tag{52}$$

Based on the previously made assumptions that both the inlet flux and contaminant concentration are constant, along with with the homogeneous distribution of the adsorbent throughout the column, it follows that the wave front will propagate with constant velocity $\hat{s}_{\hat{t}} = \hat{v}$. Consequently, the position of the wave front can be defined as $\hat{s}(\hat{t}) = \hat{v}\hat{t} + \hat{s}_0$, where $\hat{s_0}$ is a constant determined by the behavior of the fluid evolution in the initial transient. Considering this we can proceed to integrate Eq. (50), and after applying the boundary conditions at $\eta \to \infty$ defined above we obtain:

$$\hat{f} = \hat{v}\hat{q} \tag{53}$$

This solution lets us reformulate Eq. (51) in terms of $\hat{f}$ and η, leading to a differential equation that can be solved analytically:

$$\frac{\partial \hat{f}}{\partial \eta} = \frac{\hat{f}(\delta_9\delta_4 - \hat{v}) + \hat{f}^2(1 + \delta_9\delta_{45})}{\hat{v}\delta_4 + \hat{v}\delta_{45}\hat{f}}. \tag{54}$$

By applying the boundary conditions at $\eta \to -\infty$ in both previous equations, we can find two expressions for the value of the velocity $\hat{v}$ of the wave front:

$$\hat{v} = 1 + \delta_9(\delta_4 + \delta_{45}) = \frac{1}{\hat{q}_e} \tag{55}$$

If we substitute this expression in Eq. (54) and integrate it we obtain the implicit solution of $\hat{f}$ in terms of η:

$$\hat{f} - 1 = K \exp\left[\eta\left(\frac{1 + \delta_9\delta_{45}}{\hat{v}(\delta_4 + \delta_{45})}\right)\right] \hat{f}^{\delta_4/(\delta_4+\delta_{45})}, \tag{56}$$

where K is the constant of integration. Changing back to $\hat{x}, \hat{t}$ coordinates and reordering the factors we can rewrite Eq. (56) as:

$$\hat{f} - 1 = K\ \exp\left[\hat{s}_0\left(\frac{-\delta_9\delta_{45} - 1}{\hat{v}(\delta_4 + \delta_{45})}\right)\right] \exp\left[(\hat{x} - \hat{v}\hat{t})\left(\frac{1 + \delta_9\delta_{45}}{\hat{v}(\delta_4 + \delta_{45})}\right)\right] \hat{f}^{\delta_4/(\delta_4+\delta_{45})}, \tag{57}$$

where K and $\hat{s}_0$ are constant and unknown. To determine its value we will introduce a new constraint. By defining $\hat{t}_{1/2}$ as the time when the wave front leaves the column we can derive another boundary condition:

$$\hat{c}_1 = 1/2,\ \hat{f} = \delta_4/(2 - \delta_{45}), \quad \text{at} \quad \hat{t} = \hat{t}_{1/2},\ \hat{x} = \hat{L}. \tag{58}$$

As $\eta = 0$ was defined as the position where $\hat{c}_1 = 1/2$, at the same time this determines the value of $\hat{s}_0 = \hat{L} - \hat{v}\hat{t}_{1/2}$. As in experimental studies the contaminant concentration at the outlet of the column is always measured, we will usually know the value of $\hat{t}_{1/2}$. Substituting this constraint in Eq. (57) we can determine the value of the constant of integration

$$K = \left(\frac{\delta_4}{2 - \delta_{45}} - 1\right)\left(\frac{\delta_4}{2 - \delta_{45}}\right)^{-\delta_4/(\delta_4+\delta_{45})}. \tag{59}$$

Additionally, we can simplify the solution if we develop the term $\delta_4 + \delta_{45}$ as it follows:

$$\delta_4 + \delta_{45} = \frac{R_g T c_{20}}{p_a} + \frac{R_g T c_{10}}{p_a} = \frac{R_g T (c_{10} + c_{20})}{p_a} = \frac{p_0}{p_a} = 1 + \delta_3 \approx 1, \tag{60}$$

where we have used the previously developed argument that δ_3 could be neglected since it was of lower order. Taking this approximation into account we can simplify the solution:

$$\hat{f} - 1 = \hat{K_1} \exp\left[(\hat{x} - \hat{v}\hat{t})\left(\frac{1 + \delta_9\delta_{45}}{\hat{v}}\right)\right] \hat{f}^{\delta_4}, \tag{61}$$

where $\hat{K_1}$ includes all the constant terms of the equation

$$\hat{K_1} = \hat{K} \exp\left[(\hat{L} - \hat{v}\hat{t}_{1/2})\left(\frac{-\delta_9\delta_{45} - 1}{\hat{v}}\right)\right], \quad \text{with} \quad \hat{K} = -\frac{1}{\delta_4}\left(\frac{\delta_4}{2 - \delta_{45}}\right)^{\delta_{45}}.$$

At the same time, the velocity of the wave front can be rewritten as:

$$\hat{v} = 1 + \delta_9 \tag{62}$$

As $\hat{f}$ can not be isolated, we will rewrite the solution to obtain an explicit expression of $\hat{t}$ in terms of $\hat{f}, \hat{x}$:

$$\hat{t} = \frac{\hat{x}}{\hat{v}} - \frac{1}{1 + \delta_9\delta_{45}} \ln\left(\frac{\hat{f} - 1}{\hat{K_1}\hat{f}^{\delta_4}}\right) \tag{63}$$

with K_1 previously defined. Reverting the change of variables we obtain the explicit solution of $\hat{t}$ in terms of $\hat{x}, \hat{c}_1$, which reads

$$\hat{t} = \frac{\hat{x}}{\hat{v}} - \frac{1}{1 + \delta_9\delta_{45}} \ln\left(\frac{\hat{c}_1 - 1}{\hat{K_1}(\delta_4\hat{c}_1)^{\delta_4}(1 - \delta_{45}\hat{c}_1)^{\delta_{45}}}\right), \tag{64}$$

Having an explicit solution of $\hat{t}$ in terms of $\hat{c}_1$ and $\hat{x}$ will simplify plotting the breakthrough curve. If we fix $\hat{x} = \hat{L}$ we will obtain the evolution of $\hat{t}$ in terms of $\hat{c}_1$ at the end of the column, and by changing the axis we will then have the breakthrough curve. Combining Eqs. (63, 70) with Eqs. (53, 45, 47) we can compute the explicit solution of $\hat{t}$ in terms of $\hat{q}$, $\hat{u}$ and $\hat{c}_2$:

$$\hat{t} = \frac{\hat{x}}{\hat{v}} - \frac{1}{1 + \delta_9\delta_{45}} \ln\left(\frac{\hat{v}\hat{q} - 1}{\hat{K_1}(\hat{v}\hat{q})^{\delta_4}}\right) \tag{65}$$

$$\hat{t} = \frac{\hat{x}}{\hat{v}} - \frac{1}{1 + \delta_9\delta_{45}} \ln\left(\frac{1 - \hat{c}_2}{\hat{K_1}(\delta_{45}\hat{c}_2)^{\delta_{45}}(1 - \delta_4\hat{c}_2)^{\delta_4}}\right), \tag{66}$$

$$\hat{t} = \frac{\hat{x}}{\hat{v}} - \frac{1}{1 + \delta_9\delta_{45}} \ln\left(\frac{\hat{u} - 1}{\hat{K_1}(\delta_{45})^{\delta_{45}}(\hat{u} - \delta_4)^{\delta_4}}\right). \tag{67}$$

To find the solution for the pressure we have to integrate Eq. (46), obtaining

$$\hat{p} = -\hat{u}\eta + C. \tag{68}$$

If we use the pressure boundary conditions at the outlet of the column Eq. (37) combined with the constraints at $\hat{t}_{1/2}$, Eq. (58), the constant of integration is determined $C = 0$. Changing back to $\hat{x}, \hat{t}$ coordinates, the pressure solution can be written as:

$$\hat{p} = -\hat{u}(\hat{x} - \hat{v}\hat{t} - \hat{s}_0). \tag{69}$$

Note that the solution is in terms of $\hat{u}$, as we do not have an explicit expression for the velocity.

Mathematically, Eq. (70) and consequently the other solutions as they are derived from the first, hold for all values of $\hat{x}$, $\hat{t}$, and $\hat{c}_1 < 1$. This will always be satisfied as contaminant concentration will never exceed its inlet value. However, physically the expression will not hold during the initial transient, as the term $\partial\hat{c}_1/\partial\hat{t}$ in Eq. (31) will not be negligible in the incipient phase. Therefore we will restrict the travelling wave solution for $t \geqslant L/u_{in}$, once the initial stage of the process is finished.

4.2 Dimensional solution

Writing the governing equations back in dimensional form we obtain:

$$t = \frac{x}{v} - \frac{\Delta t}{1 + \frac{k_{de} R_g T}{k_{ad} p_a}} \ln\left(\frac{c_1/c_{10} - 1}{K_1 (\frac{R_g T c_{20} c_1}{p_a c_{10}})^{\frac{R_g T c_{20}}{p_a}} (1 - \frac{R_g T c_1}{p_a})^{\frac{R_g T c_{10}}{p_a}}} \right), \tag{70}$$

$$t = \frac{x}{v} - \frac{\Delta t}{1 + \frac{k_{de} R_g T}{k_{ad} p_a}} \ln\left(\frac{\frac{\Delta t v \bar{q}}{\mathcal{L} \bar{q}^*} - 1}{K_1 (\frac{\Delta t v \bar{q}}{\mathcal{L} \bar{q}^*})^{\frac{R_g T c_{20}}{p_a}}} \right), \tag{71}$$

$$t = \frac{x}{v} - \frac{\Delta t}{1 + \frac{k_{de} R_g T}{k_{ad} p_a}} \ln\left(\frac{1 - c_2/c_{20}}{K_1 (\frac{R_g T c_{10} c_2}{p_a c_{20}})^{\frac{R_g T c_{10}}{p_a}} (1 - \frac{R_g T c_2}{p_a})^{\frac{R_g T c_{20}}{p_a}}} \right), \tag{72}$$

$$t = \frac{x}{v} - \frac{\Delta t}{1 + \frac{k_{de} R_g T}{k_{ad} p_a}} \ln\left(\frac{\frac{u \Delta t}{\mathcal{L}} - 1}{K_1 (\frac{R_g T c_{10}}{p_a})^{\frac{R_g T c_{10}}{p_a}} (\frac{u \Delta t}{\mathcal{L}} - \frac{R_g T c_{20}}{p_a})^{\frac{R_g T c_{20}}{p_a}}} \right), \tag{73}$$

$$p = \frac{\Delta p}{\mathcal{L}} \left[-u \Delta t (x - vt - \mathcal{L} s_0) \right] + p_a, \tag{74}$$

where

$$K_1 = K \ \exp\left[\frac{L - v t_{1/2}}{\mathcal{L}} \left(\frac{-\mathcal{L}(\frac{k_{de} R_g T}{k_{ad} p_a} - 1)}{v \Delta t} \right) \right], \quad \text{with} \quad K = -\frac{c_{20}}{c_{10}} \left(\frac{R_g T c_{20}}{2 p_a - R_g T c_{10}} \right)^{R_g T c_{10}}$$

and $s_0 = L - v t_{1/2}$.

5 Model Results and Validation with Experimental Data

Once the model is developed and we have obtained the relations that define the evolution of the system, the predictions of the model should be compared against experimental data to see if it works correctly. As packed columns are used to filter a large variety of contaminants they can have very different adsorption mechanisms and regime flows. Therefore, the parameters that define a real system can vary a lot. To ensure that our model performs well in different scenarios we will test it with two different experimental datasets.

The first experiment is toluene adsorption using activated carbon. The resulting data is the evolution of contaminant concentration at the outlet of the column for three different inlet concentrations of contaminant. As discussed before, one of the inconsistencies that arise in adsorption models is that k_{ad} varies with the inlet concentration of contaminant, conflicting with the premise that this coefficient was constant. After determining k_{ad} for the three cases we will see if it varies with different contaminant concentrations or it remains constant.

The second experimental dataset we will use is obtained from the measurements of CO2 adsorption in activated carbon. The model that has been developed considers that the fluid may have variable velocity inside the column and consequently variable pressure. Contaminant concentrations in the previous experiment are very small and therefore the gradient of these variables throughout the column will not be appreciable. We will use the experimental data provided by this experiment to check how the model performs in a variable velocity system, and check if the evolution of these variables is as expected.

All the parameters needed to describe the system are given together with experimental data. However, k_{ad} and sometimes $\overline{q}^*$ and k_L are not known. We will obtain k_{ad} fitting the solution in Eq. (70) to the experimental data. If $\overline{q}^*$ and k_L are not given we will determine them fitting the parameters to the Langmuir isotherm, as it was discussed in Section 2.7.

5.1 Toluene adsorption using activated carbon

The data for toluene adsorption has been obtained from **dataset**. In this experimental study a gas mixture of toluene-N2, using N2 as the gas carrier, was filtered using activated carbon Norit RB3 adsorbent. The experiment was carried out at 26$^{\text{o}}$C and 1 atm. 160 mg of this adsorbent were introduced into 10 x 5.4 mm (D x L) glass column and the inlet flow was kept constant at 205 mL/min. The experimental data provided by the study is the concentration of toluene at the outlet of the column, determined by means of gas chromatography with flame ionization detector (GC-FID). The procedure was repeated for three different values of toluene concentration ranging 409, 1316 and 2835 mg/m^3. All the parameters describing the operating conditions and data of the experiment are given in Table 5.1.

Parameter	Symbol	Value
Toluene initial concentration	c_{10}	0.004, 0.014 and 0.031 mol/m^3
N_2 initial concentration	c_{20}	40.74, 40.73 and 40.71 mol/m^3
Toluene molar mass	M_1	0.092 kg/mol
N_2 molar mass	M_2	0.028 kg/mol
Temperature	T	299.15 K
Ambient pressure	p_a	101325 Pa
Adsorption saturation	$\overline{q}^*$	$-$ mol/kg
Adsorption equilibrium	$\overline{q}_e$	$-, -$ and $-$ mol/kg
Bed void fraction	ε	0.336
Bed length	L	0.0054 m
Bed radius	R	0.005 m
Diameter of bed particles	d_p	$0.212 - 0.425 \times 10^{-3}$ m
Gas viscosity	μ_g	$1.80\times10^{-5}, 1.81\times10^{-5}$ and 1.83×10^{-5} Pa s
Axial diffusion coefficient	D	$\sim 10^{-6}$
Density of adsorbed toluene	ρ_q	377.25 kg/m^3
Initial volume flux	J_{in}	3.43×10^{-6}m^3/s
Initial interstitial velocity	u_0	0.13 m/s
CO_2 adsorption rate	k_{ad}	$-$ s^{-1}
CO_2 desorption rate	k_{de}	$-$ s^{-1}

The values of the gas viscosity have been computed using the data in [8].

As we have previously assumed, the flow of the fluid through the porous media is described by Ergun's relation. Therefore, the parameters α and β can be computed as it follows:

$$\alpha = \frac{1.75(1-\varepsilon)^2}{d_p\varepsilon} \approx 1.06 \times 10^4,$$
$$\beta = \frac{150\mu_g(1-\varepsilon)^2}{d_p^2\varepsilon^2} \approx 1.07 \times 10^5, \tag{75}$$

5.1.1 Determination of missing parameters

From the data given together with the experimental dataset we already know almost all the parameters that define our system. However, there are five parameters that we still have to calculate to compute the analytical solutions and check the accuracy of the model. The five unknown parameters are $\overline{q}^*, \overline{q}_e, k_{de}, k_L$ and k_{ad}. As k_{ad} and k_{de} are related through the definition of k_L, by computing two of the three we will know the value of all of them.

Using the toluene concentration at the outlet of the column provided by the experimental data we can use Eq. (28) to numerically compute $\overline{q}_e$ for the three different inlet concentrations of toluene, obtaining

c_{in} [mg/m^3]	409	1316	2835
$\overline{q}_e$ [mol/kg]	0.241	0.310	0.353

As it was explained in Section 2.7, the Langmuir isotherm can be used to compute the saturation point of the adsorbent $\overline{q}^*$ and the adsorption coefficient k_L. As the data of the evolution of the system is available for more than one inlet concentration, we can fit Eq. (25) to the points $(\frac{1}{c_e}, \frac{1}{q_e})$, which can be computed using the data in Table 5.1.1. In Figure 2 the fitting of Eq. (25)

to the data in Table 5.1.1 can be seen. The values $k_L = 4453.53$ m^3/kg and $\overline{q}^* = 0.372$ kg/kg have been obtained.

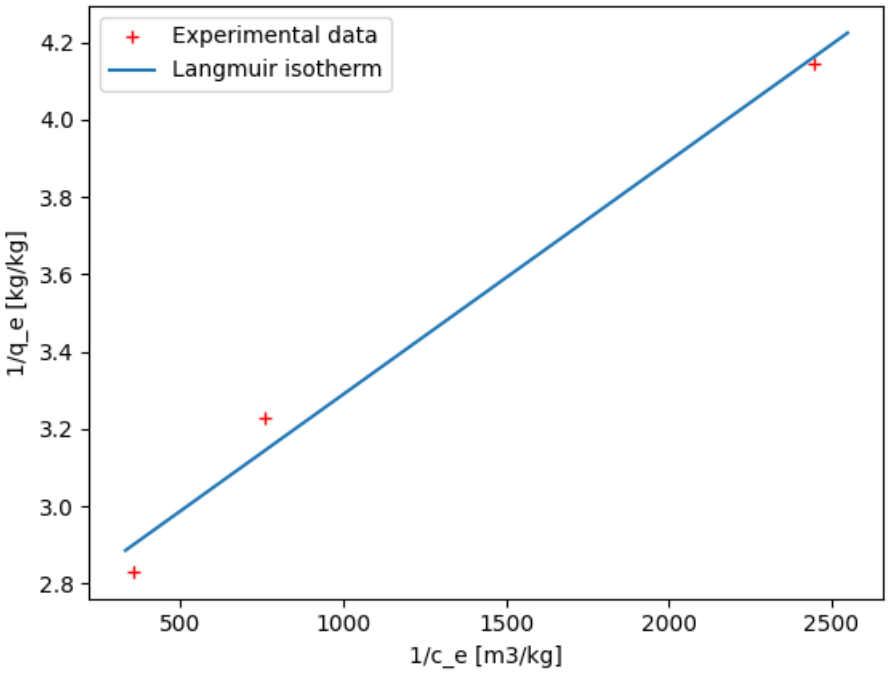

Figure 2: Fitting of the Langmuir isotherm for the toluene data.

The only parameter left to determine at this point is k_{ad}. If we revisit the solution in Eq. (70), we can see that if we plot the function $\hat{t} = \hat{t}(\hat{L}, \hat{c}_{10})$ for a range of values of c_{10} and exchange the axis, we will obtain $\hat{c}_{10} = \hat{c}_{10}(\hat{L}, \hat{t})$. This will be the evolution of contaminant concentration at the outlet of the column predicted by the analytical solution. As it predicts exactly what is given in the experimental data we will be able to perform a parameter fitting to compute the value of k_{ad}. Following the definition of k_L, the value of k_{de} will be determined simultaneously:

c_{in} [mg/m^3]	409	1316	2835
k_{ad} [m^3/kg s]	1.12	1.59	1.14
k_{de} [s^{-1}]	2.53×10^{-4}	3.62×10^{-4}	2.55×10^{-4}

With all the parameters determined we can calculate the scaling variables defined in Eq. (30) that we will use in the non-dimensionalization of the model:

c_{in} [mg/m^3]	409	1316	2835
$\mathcal{L}$ [m]	1.36×10^{-2}	9.45×10^{-3}	1.34×10^{-2}
Δt [s]	2.21×10^{3}	4.83×10^{2}	3.09×10^{2}
Δp [Pa]	1.89×10^{2}	1.31×10^{2}	1.86×10^{2}

Using the system parameters together with the scaling variables we can finally compute the dimensionless parameters that appear in the non-dimensional equations:

c_{in} [mg/m^3]	409	1316	2835
δ_1	4.73×10^{-5}	1.50×10^{-4}	2.81×10^{-4}
δ_2	5.55×10^{-4}	8.14×10^{-4}	5.74×10^{-4}
δ_3	1.87×10^{-3}	1.29×10^{-3}	1.84×10^{-3}
δ_4	1.00	1.00	0.99
δ_5	1.08×10^{-4}	3.43×10^{-4}	7.61×10^{-4}
δ_6	1.47×10^{-2}	1.47×10^{-2}	1.47×10^{-2}
δ_7	3.23×10^{-4}	1.13×10^{-3}	2.50×10^{-3}
δ_8	3.30×10^{-8}	1.66×10^{-7}	2.59×10^{-7}
δ_9	0.56	0.17	0.08

As it was discussed in Section 3.1, δ_1, δ_2 and δ_3 are indeed of lower order and therefore their obviation is now proven to be a good approximation. For this experimental set specifically, δ_5 could also be neglected. Its low value follows from the fact that the concentration of contaminant in the fluid is very low. In this case the velocity of the fluid is constant and δ_5 could be neglected. However, the model has been developed for cases where the fluid velocity will be variable. This is equivalent to saying that the model has been developed for systems with high contaminant concentration, in which this dimensionless parameter will play a significant role in the evolution of the system.

As we have mentioned, in this specific experiment the contaminant concentration is very low. Therefore, we will additionally neglect δ_7 as it was also discussed in Section 3.1.

With all the parameters determined we can plot the breakthrough curves predicted by the model and compare them with the ones obtained experimentally. As it can be seen in Figure 3, the model predictions show great agreement with experimental data.

5.1.2 Adsorption coefficient variation

As it has been discussed, the adsorption coefficient obtained from the parameter fitting should remain constant with the contaminant inlet variation. In the previous section it can be seen that k_{ad} shows a maximum variation of the 40% approximately. In Table 1 a comparison between the adsorption coefficients obtained for different models can be seen.

	c_{in} [mg/m^3]	409	1316	2835
Model 1	k_{ad} [s^{-1}]	1.12	1.59	1.14
Model 2	k_{ad} [m^3/kg s]	0.34	1.32	2.14
Model 3	k_{ad} [m^3/kg s]	1.12	1.53	1.13

Table 1: Comparison of adsorption coefficients for different models obtained from [4]. Model 1 corresponds to the model developed in this work. Models 2 and 3 correspond to constant velocity models, with linear and nonlinear mass transfer equations respectively.

Model 1 corresponds to the one developed in this work. k_{ad} for models 2 and 3 has been taken from the results in [4], where fitting has been performed for this same experimental data. Both models consider that the fluid velocity inside the column is constant. However, model 2 uses a linear mass sink equation and model 3 the same nonlinear Langmuir equation as the one used in this project to model mass transfer. Since the contaminant concentration in the experiment is low, the fluid velocity inside the column remains nearly constant. Therefore, models 1 and 3 are expected to obtain very similar outcomes as the only difference between them is that one assumes constant velocity while the other does not. This expectation aligns with the results obtained, shown in Table 1. In addition, both experiments show almost identical k_{ad} values

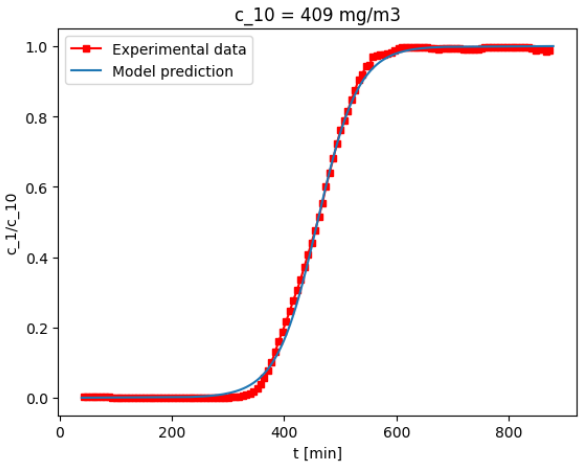

(a) $k_{ad} = 1.12$ m^3/(kg s)

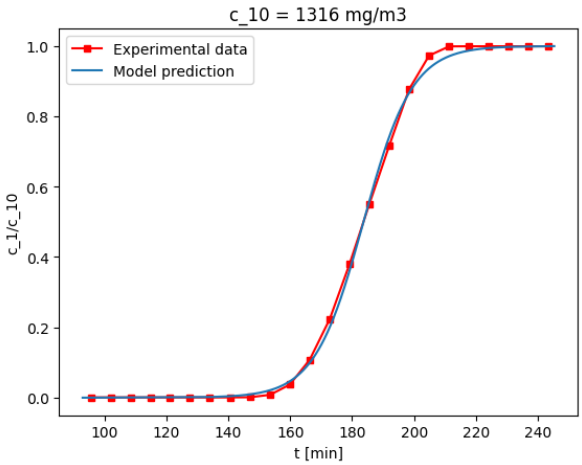

(b) $k_{ad} = 1.61$ m^3/(kg s)

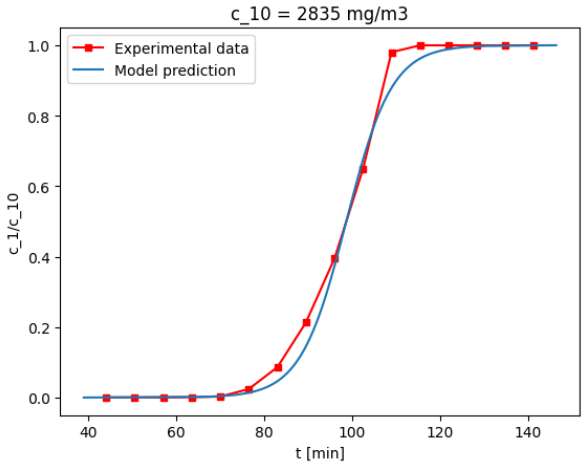

(c) $k_{ad} = 1.13$ m^3/(kg s)

Figure 3: Comparison between the breakthrough curves obtained in the toluene experiment and predicted by the model for the different inlet concentrations.

for the first and third terms. The middle term however, deviates around a 40% as mentioned before, what may be caused by an inaccuracy in the experimental study. In the linear model on the other hand, k_{ad} varies almost linearly with c_{in}. This error suggests that this model may be oversimplifying the process or making an incorrect assumption.

5.2 CO_2 adsorption using activated carbon

Throughout the previous section we have checked that the model works well, predicting with good accuracy the breakthrough curve. However, as the contaminant concentration was small, the velocity of the fluid, pressure and carrier concentration remained constant during the whole process and we were not able to check if the model predicted the evolution of these quantities correctly. In this section we will test the model with a new dataset, taken from an experimental study uses a higher amount of inlet contaminant. In this case the contaminant volume fraction is around 15%, much higher than the 1.08×10^{-4}%, 3.43×10^{-4}% and 7.61×10^{-4}% of the previous experiment. With this amount of inlet contaminant, the carrier concentration, pressure and velocity will vary along the column as contaminant is removed, and we will be able to test the evolution of these variables predicted by the model.

The experiment involves the filtering of a gas composed by CO_2 and N_2. The fluid is confined through a packed column of activated carbon, which will remove the CO_2 by adsorption. The data of the experiment is shown in Table 5.2.

Parameter	Symbol	Value
CO_2 initial concentration	c_{10}	6.03 mol/m^3
N_2 initial concentration	c_{20}	34.17 mol/m^3
CO_2 molar mass	M_1	0.044 kg/mol
N_2 molar mass	M_2	0.028 kg/mol
Temperature	T	303.15 K
Ambient pressure	p_a	101325 Pa
Adsorbent saturation	$\overline{q}^*$	1.57 mol/kg
Adsorbent equilibrium	$\overline{q}_e$	− mol/kg
Adsorbent density	ρ_s	1818 kg/m^3
Bed void fraction	ε	0.56
Bed length	L	0.2 m
Bed radius	R	0.005 m
Diameter of bed particles	d_p	6.5×10^{-4} m
Gas viscosity	μ_g	1.76×10^{-5} Pa s
Axial diffusion coefficient	D	2.57×10^{-5}
Density of adsorbed CO_2	ρ_q	325 kg/m^3
Initial volume flux	J_{in}	8.33×10^{-7}m^3/s
Initial interstitial velocity	u_0	0.019 m/s
CO_2 adsorption rate	k_{ad}	− s^{-1}
CO_2 desorption rate	k_{de}	− s^{-1}

As we did in the previous section we can compute α and β coefficients:

$$\alpha = \frac{1.75(1-\varepsilon)^2}{d_p \varepsilon} \approx 2.11 \times 10^3,$$
$$\beta = \frac{150\mu_g(1-\varepsilon)^2}{d_p^2 \varepsilon^2} \approx 3.86 \times 10^3. \tag{76}$$

Again we can numerically compute $\hat{q}_e$ with Eq. (28). In this case we do not have directly the quantity of adsorbent inside the column, but we can compute it using the adsorbent density:

$$M_{at} = \frac{\delta_4 - \delta_{45}}{c_{10}\left(\frac{1}{\hat{q}_e} - 1\right)} = \rho_s * \pi * R^2 * L * (1-\varepsilon) = 0.016 \text{ kg}, \tag{77}$$

obtaining $\overline{q}_e = 0.28$ mol/kg. With $\hat{q}_e$ determined, the next step would be to use the Langmuir isotherm to compute k_L and $\overline{q}^*$. However, this experiment was only performed with one inlet concentration so we can not compute the linear regression as we only have one $(\frac{1}{c_e}, \frac{1}{q_e})$ point. Nevertheless, we already know the value of $\hat{q}^*$ as it is provided together with the experimental data. k_L on the other hand can be alternatively computed revisiting the definition of velocity in Eq. (55). A second and equivalent expression for the front wave velocity can be obtained if we impose the boundary conditions for $\eta \to -\infty$ in Eq. (53):

$$\hat{v} = \frac{1}{\hat{q}_e} \tag{78}$$

Combining both of them and using the definition of δ_9 we obtain an alternative expression for k_L:

$$k_L = \frac{1}{c_{10}\left(\frac{1}{\hat{q}_e} - 1\right)} \tag{79}$$

Using the data in Table 5.2 we can compute the Langmuir constant takes the value $k_L = 0.036$ m^3/mol. With all the parameters defined we can again perform a fitting using the breakthrough curve provided by the experimental data to determine $k_{ad} = 0.0025$ m^3/(mol s), $k_{de} = 0.069$ s^{-1}.

After determining the value of all the quantities that describe the system we can compute the scaling variables and the dimensionless parameters:

$$\mathcal{L} = 0.021 \text{ m}, \quad \Delta t = 41.46 \text{ s}, \quad \Delta p = 1.54\text{Pa}$$

$$\delta_1 = 1.67 \times 10^{-2}, \quad \delta_2 = 6.44 \times 10^{-2}, \quad \delta_3 = 1.52 \times 10^{-5}, \quad \delta_4 = 0.85, \quad \delta_5 = 0.18$$
$$\delta_6 = 9.94 \times 10^{-3}, \quad \delta_7 = 0.28, \quad \delta_8 = 3.78 \times 10^{-5}, \quad \delta_9 = 4.61$$

As it happened in the previous experiment, the first three dimensionless parameters are of lower order and therefore neglecting them was a good approximation. In contrast, δ_5 now should not be neglected. This implies that the carrier concentration will vary significantly throughout the column, what matches with the fact that we have a higher contaminant concentration that will be adsorbed. In Eq. (35), the δ_7 term will be the leading one as δ_6 and δ_8 will be of lower order, as we expected for cases with high contaminant concentration.

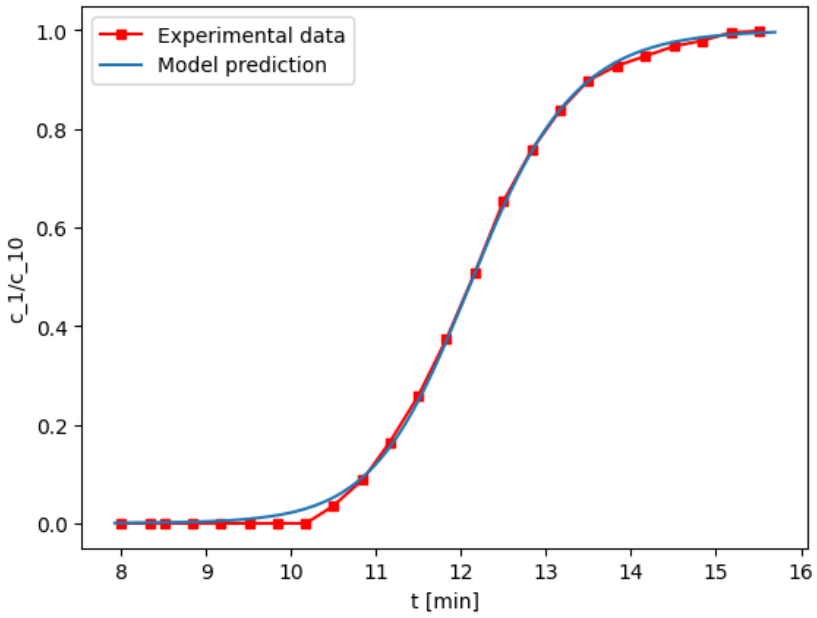

Figure 4: Comparison between the breakthrough predicted by the model and the one obtained experimentally for $k_{ad} = 0.0025$ m^3/(mol s).

5.2.1 Model validation and comparison with experimental data

Figure 4 shows the comparison of the breakthrough curve predicted by the model and the one obtained experimentally. As it can be observed, the model prediction shows great agreement with the experimental data, following the experimental data profile during most of the process. The only region where the model prediction deviates a little is when contaminant first reaches the outlet of the column. The model predicts a gradual increase on the contaminant concentration while experimentally increases more sharply.

In Figure 5 we can see the breakthrough curve including the evolution of the different variables that describe the system. Although no experimental data is available to check the validity of the result, the solutions obtained align perfectly with the physical expected outcomes. CO_2 concentration starts at $\hat{c}_1 = 0$, since the column is adsorbing it before it reaches the output. Eventually, the adsorbent saturates and contaminant moves forward until it reaches the outlet. Over time, adsorbed quantity at the outlet increases until reaching its equilibrium value $\hat{q}_e$, where adsorption and desorption equalize, and contaminant concentration reaches its inlet value $\hat{c}_1 = c_1/c_{10} = 1$.

The concentration of N_2 also evolves as expected. The normalization constant c_{20} is the concentration of N_2 measured before the gas enters the column. Therefore, when the volume fraction of the contaminant in the gas is the same as at the column inlet, N_2 concentration is $\hat{c}_2 = 1$. When contaminant is removed, the carrier gas fills the space previously occupied by the contaminant, thereby increasing its concentration. Consequently, until no contaminant reaches the outlet of the column, the concentration of the carrier gas will remain greater than 1. As the contaminant begins to pass through, the concentration gradually decreases until it reaches 1, as the amount of contaminant exiting the will be equivalent to the amount entering the column.

On the other hand, the gas velocity is directly related to the inlet flow rate of the gas, which remains constant in this scenario. However, by removing a portion of the gas, the total gas volume within the column decreases. Consequently, the gas velocity must decrease to maintain

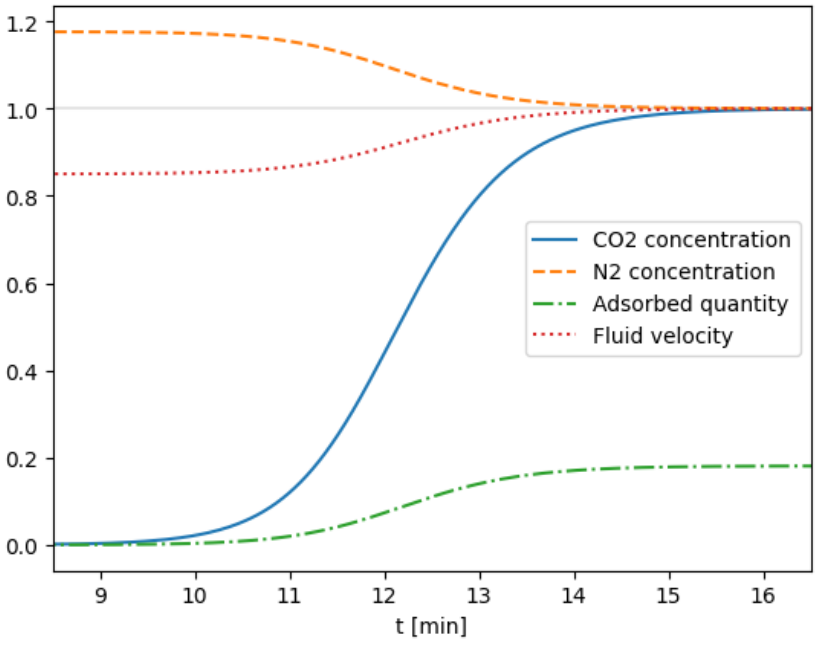

Figure 5: Evolution of CO_2, N_2 concentration, velocity and adsorbed quantity at the outlet of the column. Shown values are normalized to be able to expose them at the same time in a coherent way.

the conservation of mass. As the column saturates, contaminant and therefore velocity increase until reaching their inlet values. Pressure is not plotted as it takes a constant value $p = p_a$ at $x = L$, defined in the boundary conditions.

However, the model fails to predict the values of the variables along the column for a specific time. Figure 6 shows the state of the column at $\hat{t} = 0.9\hat{t}_{1/2}$. As it can be seen, the fluid velocity and both concentrations are different from their inlet values at $\hat{x} = 0$, where they are supposed to be $\hat{c}_1, \hat{c}_2, \hat{u} = 1$. This could be caused by an erroneous value of the front wave velocity. The model's analytical solution is a wave corresponding to the contaminant concentration at each point in space (see Figure 1b). This wave travels as adsorbent saturates at a velocity determined by the boundary conditions, given in Eq. (55). In the fitting where k_{ad} is determined, the wave function is forced to take the experimental values measured at the outlet of the column. In other words, k_{ad} determines the width of the wave. If the wave velocity computed is high, k_{ad} determined will widen the wave so that the values of contaminant concentration at the outlet of the column still meet with the experimental data. If the wave velocity is low, k_{ad} will narrow the wave function so that the values at the output are maintained. Therefore, the predicted values at $x = L$ will be correct, but if the front velocity computed is wrong, the wave will be too wide or narrow and the model output values inside the column will be wrong.

We can therefore conclude that the error arises with the wave velocity. No errors seem to be committed in the procedure followed to obtain Eq. (55), so the problem must be related with the constants involved to compute it. Revisiting Eq. (55), we can see that $\hat{v}$ only depends on δ_9, which at the same time depends on k_L. Therefore, the issue might be related with Eq. (28) used to numerically compute $\overline{q}_e$, as its value is abnormally low for an experiment of these characteristics. $\overline{q}_e$ is used to compute k_L, and if it had a higher value the front velocity would be lower and the wave would narrow, solving the problem. We could also consider the scaling variables $\mathcal{L}$ and Δt, which will also have an effect on the final value of the wave speed. However, the parameters used to compute them are given together with the experimental data so their values are probably correct if the parameters given are also correct.

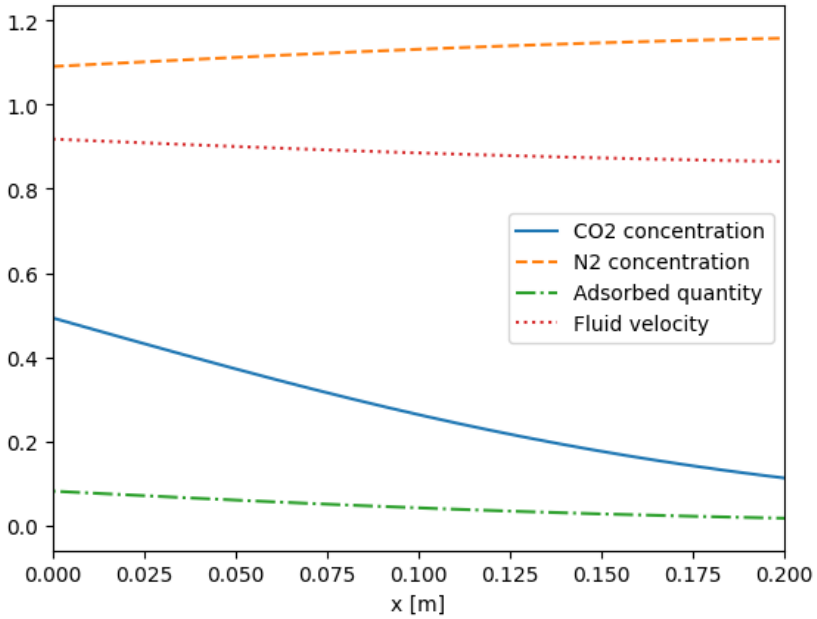

Figure 6: Concentrations of contaminant $\hat{c}_1$ and carrier $\hat{c}_2$, adsorbed quantity $\hat{q}_L$ and fluid velocity $\hat{u}$ throughout the column at $\hat{t} = 0.9\hat{t}_{1/2}$.

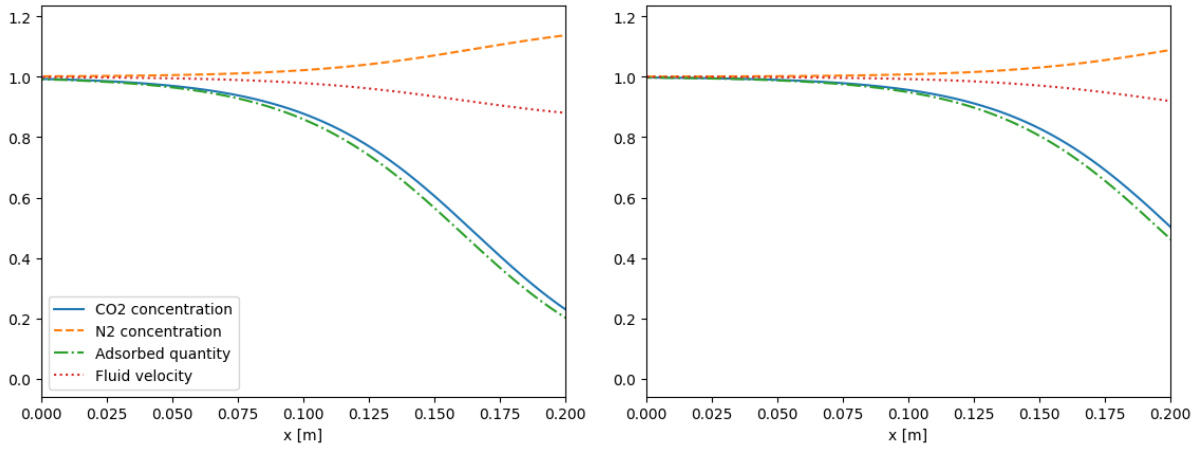

(a) **(b)**

Figure 7: Concentrations of contaminant $\hat{c}_1$ and carrier $\hat{c}_2$, adsorbed quantity $\hat{q}_L$ and fluid velocity $\hat{u}$ throughout the column if desorption is neglected. On the left for $t = 0.9\,t_{1/2}$, and for $t = t_{1/2}$ on the right.

If the desorption process is obviated, adsorbed quantity once the equilibrium is reached will be $\overline{q}_e = \overline{q}^*$ so $\hat{q}_e = 1$. Introducing this in Eq. (79), we can see that the Langmuir constant will tend to infinity. Physically, this means that the adsorbent will have more capacity and therefore the velocity of the front wave will be lower. Following the reasoning developed previously, if the velocity decreases the wave will narrow. In Figure 7a the state of the column under this conditions is shown for $t = 0.9\,t_{1/2}$. As it can be observed, results are now more coherent. At $\hat{x} = 0$, the system variables are $\hat{c}_1$, $\hat{c}_2$, $\hat{u} = 1$, corresponding with their inlet values. The adsorbed quantity is also $\hat{q} = 1$, as the adsorbent in the inlet region has already saturated for this value of t. As we move forward in the column contaminant decreases, since adsorbent is not saturated yet. The contaminant drop is followed by an increase in the carrier concentration and a decrease in the fluid velocity. This behaviour of the variables fits perfectly with the physical outcomes expected, as discussed above. For bigger values of t we can see how the wave travels forward in the column, as it is shown in Figure 7b.

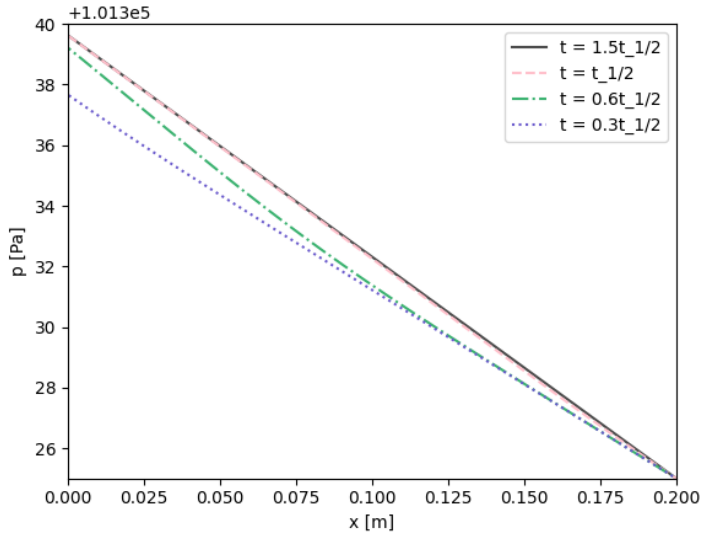

Figure 8: Pressure evolution along the column for different values of time.

In Figure 8, pressure variation along the column can be observed. The dark line is the pressure computed at $\hat{t} = 1.5\,\hat{t}_{1/2}$. For this value of $\hat{t}$ the column has saturated and the fluid passes through unchanged. Hence, there is no velocity gradient and pressure variation matches with the pressure profile when no material is being adsorbed. For lower values of $\hat{t}$ when adsorption occurs, in regions where mass transfer is higher pressures computed are further from the pressure profile at $\hat{t} = 1.5\,\hat{t}_{1/2}$. This aligns with the expected output: adsorption decreases the amount of substance of the fluid and consequently the pressure.

5.2.2 Comparison with constant velocity models

Throughout the discussion carried with the previous experiment we have seen that models using linear mass transfer equations do not work as good as models using nonlinear mass transfer equations. In this section we will compare the model developed in this work with a constant velocity model, and discuss if the difference on the result is relevant. The governing equations of the constant velocity model are computed in [4]. The model is equivalent to the one developed in this paper, but considering constant fluid velocity. For this comparison we have neglected desorption in both of them to solve the problem related to $\hat{q}_e$.

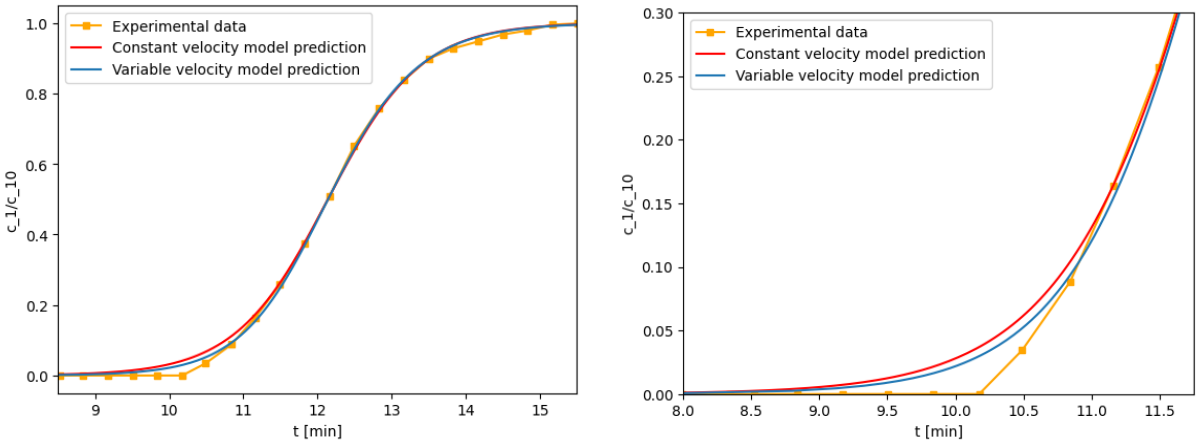

Figure 9: Comparison of the breakthrough curves predicted by the constant velocity model in green and by the variable velocity model in blue together with the experimental data. The right figure shows the amplified view of the most diverging region between the two models.

Figure 9 shows the breakthrough curves predicted by the two models, which have a very similar profile. However, the variable velocity model is more accurate when $t < 0.9t_{1/2}$. This aligns with the expected result. As it can be seen in Figure 7, the fluid's velocity is smaller than its inlet value for $t < 0.9t_{1/2}$. At $t = 0.9t_{1/2}$, fluid velocity starts increasing until reaching its inlet value. Following this reasoning it is clear that the constant velocity model will have more error in the region where the fluid velocity differs the most from its inlet value, $t < 0.9t_{1/2}$, as $\hat{u} = \hat{u}_{in}$ is the value considered by the constant velocity model.

6 Conclusions

In this work a mathematical model to describe contaminant adsorption in packed columns has been developed. The contaminant was assumed to be part of a two component fluid, traveling in a porous media embedded in a cylindrical column. The governing equations were developed using a non-linear mass transfer equation and considering variable velocity, what is a new contribution to the field. The process was assumed to be isothermal, although this could be an erroneous approximation in some situations. Through non-dimensionalisation the system was reduced, neglecting terms with a smaller relative size that would have been irrelevant on the evolution of the system.

Once the reduction was applied, an analytical wave solution has been computed. The traveling wave solution captures the evolution of the system accurately, once an initial transient was completed. Although predicting the values of the breakthrough curve, the velocity of the wave computed for the second experiment was proven to be wrong. This manifested when computing the evolution of the variables on inner points of the column. The error was probably produced during the computation of the equilibrium adsorbed quantity, either because the numerical method proposed was invalid or a parameter given with the experimental data was not correct. Remains pending to correct this error. To be able to study the model with the second experiment, desorption was neglected, what defined a new value for $\overline{q}_e = \overline{q}^*$ and solved the error.

With the solutions provided, the evolution of the concentrations of the two components of the gas, the pressure, velocity and adsorbed quantity could be computed at any point of the column. The solution was tested with different datasets of contaminant capture on activated carbon adsorbent. Missing parameters were found fitting the solution to the experimental data. In systems with low contaminant concentration, the model predictions could not be distinguished form constant model predictions, as velocity inside the column barely varied. The second experiment used to validate the model employed around 15% of contaminant volume fraction. In cases with more contaminant, as it would be the case with gas pollutants in exhaust pipes, the model exhibited a slightly better performance than a constant velocity model. A case with more pollutant concentration could be studied to test if considering variable velocity can be truly relevant in some cases. In all experiments the model predicted the breakthrough curve matching the experimental data with high accuracy.

All the solutions are presented as explicit functions of t, as the explicit expression for the variables could not be computed. Nevertheless this problem should be easily overcomed with simple numerical approaches. As these solutions have proven to represent correctly the process, they could help understand better how do parameters affect adsorption in packed columns and could be used to improve this technology and its implementation.

Acknowledgments

Acknowledgements to my director and supervisor Timothy Myers for helping me throughout the project. Thanks to my family, for their support and for encouraging me to do my best. Acknowledgements to my colleagues for making this year an amazing experience. Last, special thanks to Alba, without who I probably wouldn't be writing these final words. I believe this project reflects part of what I have learned during these years at the university, and I hope to make the people who know me best feel proud about the work done here.

References

[1] Hannah Ritchie and Max Roser, 'Air pollution,' https://ourworldindata.org/air-pollution, 2017.

[2] Ben P. Harvey, Sylvain Agostini, Shigeki Wada, Kazuo Inaba and Jason M. Hall-Spencer, 'Dissolution: The achilles' heel of the triton shell in an acidifying ocean,' https://doi.org/10.3389/fmars.2018 2018.

[3] Zhe Xu, Jian-guo Cai and Bing-cai Pan, 'Mathematically modeling fixed-bed adsorption in aqueous systems,' J. Zhejiang Univ. Sci. A 14, 155–176 (2013). https://doi.org/10.1631/jzus.A1300029, 2013.

[4] Timothy G. Myers, Alba Cabrera-Codony, Abel Valverde, 'On the development of a consistent mathematical model for adsorption in a packed column (and why standard models fail),' https://doi.org/10.1016/j.ijheatmasstransfer.2022.123660, 2023.

[5] T.G. Myers, F. Font, M.G. Hennessy, 'Mathematical modelling of carbon capture in a packed column by adsorption,' 10.1016/j.apenergy.2020.115565, 2020.

[6] T.G. Myers, F. Font, 'Mass transfer from a fluid flowing through a porous media,' International Journal of Heat and Mass Transfer, 163, 120374, 2020.

[7] Mohammad Saleh Shafeeyan, Wan Mohd Ashri Wan Daud, Ahmad Shamiri, and Nasrin Aghamohammadi, 'Modeling of carbon dioxide adsorption onto ammonia-modified activated carbon: Kinetic analysis and breakthrough behavior,' Energy Fuels 2015, 29, 10, 6565–6577, 2015.

[8] Fernando J. V. Santos, Carlos A. Nieto de Castro, John H. Dymond, Natassa K. Dalaouti, Marc J. Assael, and Akira Nagashim, 'Standard reference data for the viscosity of toluene,' Journal of Physical and Chemical Reference Data 35, 1 (2006), 2006.